BJR

https://doi.org/10.1259/bjr.20201114

Received: 10 September 2020 | Revised: 19 January 2021 | Accepted: 03 February 2021

Cite this article as:
Razik A, Das CJ, Sharma R, Malla S, Sharma S, Seth A, et al. Utility of first order MRI-Texture analysis parameters in the prediction of histologic grade and muscle invasion in urinary bladder cancer: a preliminary study. *Br J Radiol* 2021; **94**: 20201114.

FULL PAPER

Utility of first order MRI-Texture analysis parameters in the prediction of histologic grade and muscle invasion in urinary bladder cancer: a preliminary study

[1]ABDUL RAZIK, MD, DNB, [1]CHANDAN J DAS, MD, DNB, FICR, FRCP, [1]RAJU SHARMA, MD, MAMS, FICR, [1]SUNDEEP MALLA, MD, DNB, [1]SANJAY SHARMA, MD, DNB, FRCR, [2]AMLESH SETH, MS, MCh and [1]DEEP NARAYAN SRIVASTAVA, MD, FAMS, FICR

[1]Departments of Radiology, All India Institute of Medical Sciences, Ansari Nagar, New Delhi, India
[2]Departments of Urology, All India Institute of Medical Sciences, Ansari Nagar, New Delhi, India

Address correspondence to: Dr Chandan J Das
E-mail: *dascj@yahoo.com*

Objective: To explore the utility of first-order MRI-texture analysis (TA) parameters in predicting histologic grade and muscle invasion in urinary bladder cancer (UBC).
Methods: After ethical clearance, 40 patients with UBC, who were imaged on a 3.0-Tesla scanner, were retrospectively included. Using the TexRAD^{TM} platform, two readers placed freehand ROI on the sections demonstrating the largest dimension of the tumor, evaluating only one tumor per patient. Interobserver reproducibility was assessed using the intraclass correlation coefficient (ICC). Mann–Whitney *U* test and ROC curve analysis were used to identify statistical significance and select parameters with high class separation capacity (AUC >0.8), respectively. Pearson's test was used to identify redundancy in the results.
Results: All texture parameters showed excellent ICC. The best parameters in differentiating high and low-grade tumors were mean/ mean of positive pixels (MPP) at SSF 0 (AUC: 0.897) and kurtosis at SSF 5 (AUC: 0.828) on the ADC images. In differentiating muscle invasive from non-muscle invasive tumors, mean/ MPP at SSF 0 on the ADC images showed AUC >0.8; however, this finding resulted from the confounding effect of high-grade histology on the ADC values of muscle invasive tumors.
Conclusion: MRI-TA generated few parameters which were reproducible and useful in predicting histologic grade. No independent parameters predicted muscle invasion.
Advances in knowledge: There is lacuna in the literature concerning the role of MRI-TA in the prediction of histologic grade and muscle invasion in UBC. Our study generated a few first-order parameters which were useful in predicting high-grade histology.

INTRODUCTION

Urinary bladder cancer (UBC) has high prevalence, largely attributable to the high 5 year survival rate of 60–80%.[1] Typically, these patients undergo multiple treatment sessions and long-term follow-up with cystoscopy. These factors result in high medical costs along with physical and emotional toll on the patients.[2,3]

The treatment of UBC occurs in multiple stages.[4] Once a neoplastic bladder mass is suspected on imaging, a transurethral resection of the bladder tumor (TURBT) is performed along with deep muscle biopsy to assess histologic grade and presence of muscle invasion. This treatment would generally suffice for patients with low-grade non-muscle invasive disease, who are then kept on follow-up cystoscopy. Patients with high-grade non-muscle invasive tumors are subjected to restage TURBT for ensuring absence of residual tumor. If muscle invasion is present at the time of the initial TURBT, then the patient proceeds to radical cystectomy, 6–8 weeks after the TURBT. Both TURBT and cystoscopy, being invasive procedures, entail risks of bleeding, perforation and sepsis in addition to anesthesia-related complications.[5]

Prediction of muscle invasion and histologic grade on imaging could help in streamlining treatment protocols so that patients can directly proceed to definitive surgery (TURBT or radical cystectomy). At present, the Vesical Imaging-Reporting and Data System (VI-RADS) provides a scoring system on multiparametric MRI to help differentiate muscle-invasive from non-muscle tumors based on morphologic parameters. VI-RADS has been validated and found to have good diagnostic performance.[6] Simple ADC

quantification on diffusion-weighted imaging (DWI) is a useful tool in predicting histologic grade.[7]

There exists an unmet need for additional quantitative tools which could improve the diagnostic performance of MRI in predicting muscle invasion and histologic grade. Texture analysis (TA) is one such tool which can be retrospectively applied to medical images for the assessment of tumor heterogeneity at the pixel level. TA has been hypothesized to predict histologic grade and early treatment response.[8] Several studies have assessed TA on CT images to predict muscle invasion and histologic grade in UBC.[9–11] However, MRI, with its higher intrinsic tissue contrast, enables better differentiation of cancerous tissue from the bladder wall than CT, and provides several vistas for the assessment of tumor morphology and physiology. Hence, TA on MRI is expected to yield more robust results than CT. Few studies have assessed radiomics on MRI in predicting tumor stage and muscle invasion.[12–15] However, these studies assessed several higher-order texture parameters which involve analysis of large volumes of data that are too complex and computationally intensive for routine purposes, apart from the question of reproducibility across different scanners and acquisition parameters. Also, beyond big data, the biological basis for these higher-order parameters is largely unknown. Hence, this study explored the potential of first-order MRI-TA parameters in predicting histologic grade and muscle invasion in UBC.

METHODS

Patient selection

After approval from the institutional ethics committee, this retrospective study included 52 consecutive patients who were subjected to dedicated pelvic MRI for suspected UBC between January 2014 and April 2016 and had urothelial cancer on subsequent histopathology. Since all the MRI were acquired several years prior to the study, informed consent was waived. Six patients, whose surgery was delayed beyond 1 month from the MRI, were excluded since the delay potentially compromised comparability between MRI and histopathology. Another six patients were excluded since their tumors were too small (<1 cm in maximum dimension) to draw a satisfactory ROI. Thus, 40 patients were available for TA. Among these, 34 patients were also part of a previous published study that assessed the utility of UBC stalk morphology and quantitative ADC on DWI to predict muscle invasion and histologic grade, respectively.[16] Although there is some overlap in the patient population between the two studies, the techniques used (TA *vs* simple mean ADC estimation) and the methods of ROI placement were completely different.

MRI protocol

Prior to the MRI, patients were asked to fast for 6 h and refrain from voiding for 2 h to ensure distension of the urinary bladder. The MRI were acquired on a 3.0-Tesla scanner (Achieva, Philips Healthcare, Best, The Netherlands), using a 16-channel phased array torso coil. The acquired sequences included turbo spin echo T_1 weighted imaging (T_1WI), fat-suppressed T_2 weighted imaging (T_2WI) and diffusion-weighted imaging (DWI) in the standard axial plane. T_2WI and DWI were also acquired in an additional orthogonal plane depending on the tumor location (coronal plane for tumors based on the superior, inferior and lateral walls; sagittal plane for tumors arising from the anterior and posterior walls). DWI was acquired using fat-suppressed echoplanar imaging under navigator-triggered respiratory gating and b-values of 0, 500, 1000 and 1500 s/mm^2 were used. After acquisition, the corresponding ADC maps were autogenerated on a pixel-by-pixel basis. Contrast-enhanced imaging was not performed as a significant number of patients had deranged renal function. The acquisition parameters are detailed in Table 1. Two sample cases are shown in Figures 1 and 2.

Texture analysis

Two radiologists (A.R. and S.M., both with 6 years of experience in general radiology) performed TA independently. Both were blinded to each other's TA-derived data as well the histopathologic reports. For TA, the images used were axial fat-suppressed T_2WI, DWI b1500 s/mm^2 and the corresponding ADC maps. All images were loaded onto the commercially available TexRAD^{TM} software (Feedback Plc.). The image slice showing the largest dimension of the tumor was selected for each MRI sequence and segmentation was performed using freehand 2D ROI to cover the entire tumor except the peripheral 1–2 mm. This was done to prevent erroneous results arising from inclusion of peritumoral tissue and volume averaging (Figure 3A). The central stalk (hyperintense on T_2WI and hypointense on DWI), if present, was not included while drawing the ROI, since it represented the reactive component of the tumor and not the tumor itself. If

Table 1. MRI acquisition protocol

Sequence	TR (ms)	TE (ms)	Slice thickness (mm)	No of averages	FOV (mm)	Matrix
T1 Ax	452	10	4	2	294 × 200	239 × 204
T2 FS Ax	5700	90	4	2	295 × 200	188 × 168
T2 FS Cor	5250	90	4	2	383 × 220	242 × 184
T2 FS Sag	4510	90	4	2	258 × 220	184 × 162
DWI Ax	2177	61	5	3	375 × 278	124 × 92
DWI Cor	2683	60	4	2	258 × 220	184 × 162
DWI Sag	2372	59	5	3	220 × 220	73 × 72

Ax, axial; Cor, coronal; DWI, diffusion-weighted imaging; FOV, field-of-view; FS, fat-suppressed; Sag, sagittal; TE, echo time; TR, repetition time; mm, millimeters; ms, milliseconds.

Figure 1. 67-year-old male with high-grade, non-muscle invasive urothelial carcinoma. (A) Axial T_2 weighted images showing a polypoidal, T2-intermediate mass arising from the left posterolateral wall of the urinary bladder, in close proximity to the vesicoureteric junction. The mass has a central T2-hyperintense stalk (*asterisk*), which was excluded while placing the ROI. (B) Axial DWI b1500 images showing intense diffusion restriction within the tumor, whereas the central stalk is hypointense (*asterisk*). DWI, diffusion-weighted imaging; ROI, region of interest.

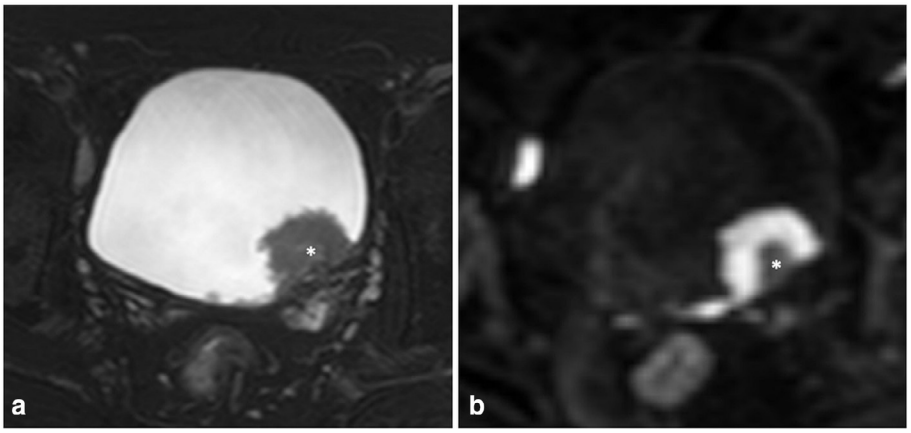

multiple tumors were present in a patient, only the largest tumor was assessed. Care was taken to avoid sections showing necrosis or hemorrhage, and in such cases, the next best slice was considered for ROI placement. We did not use 3D volumetric (whole-tumor) ROI or analysis of the adjacent healthy bladder wall in this study.

After confirmation of the ROI placement, the TexRAD^{TM} software used a Laplacian of Gaussian spatial band-pass filter to mitigate photon noise and enhance features corresponding to the spatial scale factors (SSF) applied. Five such SSF were utilized, ranging from 2 to 6 mm (hereafter labeled as SSF 2–6). The unfiltered base images (SSF 0) also underwent TA. Following this, for each SSF, the software generated a histogram representing the distribution of signal intensities across pixels and derived the following first-order texture features: mean (average grayscale intensity), standard deviation (SD; dispersion or spread of intensities relative to the mean), entropy (disorder in the distribution of the intensities), mean of positive pixels (MPP), skewness (asymmetry of the histogram), and kurtosis (peakedness of the histogram). This resulted in 36 texture parameters being generated for each ROI (Figure).

Statistical analysis

Statistical analysis was performed using XLSTAT Premium, v. 2019.1.2 for windows (Addinsoft, NY). To ensure reproducibility of all the six TA features derived by the two readers, intraclass correlation coefficient (ICC) was used. Only the texture features with ICC >0.8, suggestive of excellent interobserver agreement, qualified for the subsequent analysis.

Histopathology was used as the reference standard to classify tumors as muscle invasive or non-muscle invasive and high-grade or low-grade. To assess for any difference between the texture parameters of high-grade from low-grade tumors and

Figure 2. 60-year-old male with high-grade, muscle invasive urothelial cancer. (A) Axial T_2 weighted images showing an irregular plaque-like mass arising from the anterior and both lateral walls of the urinary bladder. The bladder is poorly distended secondary to the tethering effect of the tumor on the bladder wall. (B) Axial DWI b1500 images showing marked diffusion restriction of the tumor. DWI, diffusion-weighted imaging.

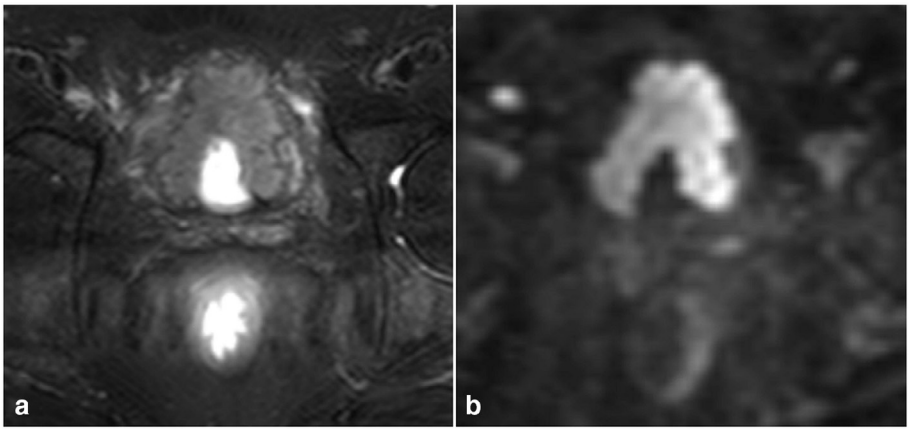

Figure 3. Texture analysis in a 60-year-old male with high-grade, muscle invasive urothelial cancer (same patient as in Figure 2). (A) Placement of a free-hand polygonal 2D ROI (outlined in blue colour) on the axial DWI b1500 slice containing the maximum viable component of the tumor, avoiding the peripheral 1–2 mm. (B, C and D) Display of the filtered images at spatial scale factors of 2 mm, 4 mm and 6 mm, respectively. DWI, diffusion-weighted imaging; ROI, region of interest

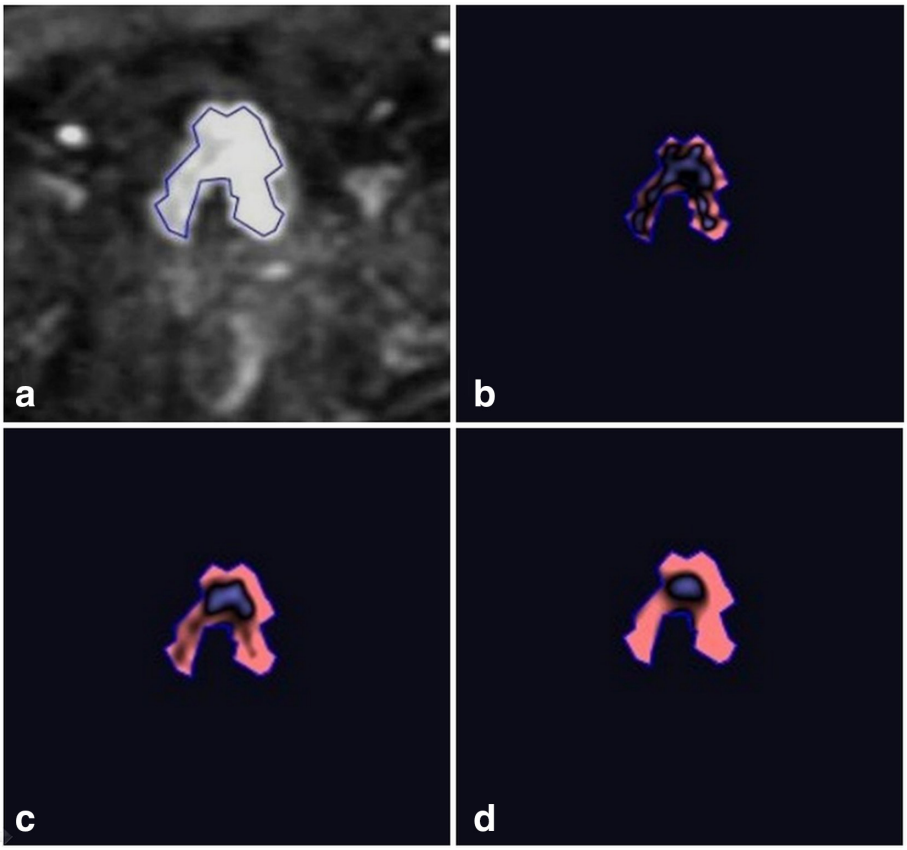

muscle-invasive from non-muscle-invasive tumors, the Mann–Whitney *U* test was applied and a p-value < 0.05 was defined as significant. Following this, ROC curve analysis was performed for all the parameters that showed significant p-value and AUC values were derived. Only the parameters that showed AUC >0.8, suggestive of high class separation capacity, were listed out in the final results. In addition, since some of the texture parameters are known to correlate with each other and introduce redundancy in the results, all the features with AUC >0.8 underwent the Pearson's product–moment correlation test to look for any mutual correlation. The Pearson's test was also used to assess any correlation between the texture parameters of high-grade tumors and muscle invasive tumors in order to negate the confounding effect of high-grade histology in the prediction of muscle invasion.

RESULTS

Patient demographics

The study population included 40 patients, among whom a large majority were males (n: 35/40, 87.5%). The group aged between 31 and 81 years, with the mean age being 57.6 ± 11.8 years. Most patients belonged to the seventh decade of life (n: 15/40; 37.5%). 22 patients (55%) were initial presenters and 18 had recurrent disease after prior treatment for UBC. The most common presenting symptom was hematuria (n: 31/40; 77.5%), followed by increased frequency of micturition (n: 2/40). Two patients had both symptoms, whereas the remaining five were asymptomatic and the disease was picked up on follow-up cystoscopy after prior treatment for UBC. The mean duration of symptoms at presentation was 16.8 ± 14.8 weeks (range: 5 days–4 years). The study group of 40 patients had a total of 86 tumors, with the majority having single tumor (n: 25/40; 62.5%). The remaining 15 patients had multifocal disease, with a mean of 2.2 tumors (range: 2–11 tumors) per person. However, for the purpose of the study, only the largest lesion was taken into account for TA. Thus, 40 tumors were evaluated. The mean size of the evaluated tumors was 3.2 ± 1.8 cm (range: 1.0–10.6 cm). After histopathological examination, all the tumors were proven to be urothelial cancer. 29 patients (72.5%) had high-grade tumors and 11 (27.5%) had low-grade tumors. 25 patients (62.5%) had non-muscle invasive disease and 15 (37.5%) showed muscle invasion. All the patients with muscle invasive disease had high-grade tumors and underwent radical cystectomy.

Interobserver correlation of texture values

All the measured texture parameters showed excellent interobserver correlation (ICC >0.8) between the two readers, with the highest correlation seen for entropy (ICC: 0.9573) (**Table 2, Figure 4**). This ensured reproducibility of the TA-derived parameters. The subsequent discussion is based on the texture parameters generated by the first reader (A.R., chosen randomly).

Table 2. ICC for the measurements extracted by the two readers (R1 and R2) for each of the six texture features

Parameter	Correlation coefficient
Mean	0.9428
SD	0.9558
Entropy	0.9573
MPP	0.9513
Skewness	0.8920
Kurtosis	0.8177

ICC, intraclass correlation coefficient; MPP, mean of positive pixels; SD, standard deviation.

Prediction of histologic grade

A total of 13 parameters (four on T_2WI, two on DWI b1500 and 7 on the ADC images) showed statistical significance (p-value < 0.05) in differentiating high-grade from low-grade tumors on the Mann–Whitney U test (Table 3). On ROC curve analysis, only three among these showed AUC >0.8 (Table 4). These parameters were (a) mean/ MPP at SSF 0 (AUC: 0.897; 95% CI: 0.759–0.970; optimal cut-off:<963.479 x 10^{-3} mm^2/s), and (b) kurtosis at SSF 5 (AUC: 0.828; 95% CI: 0.675–0.928; optimal cut-off:>−0.579); both on the ADC images. Among these, mean and MPP had exactly the same values since ADC maps contain only positive pixels. This was proven by perfect linear correlation (r: 1.0) between these parameters. On the other hand, no correlation was observed between mean/ MPP at SSF 0 and kurtosis at SSF 5 on the ADC images (r: −0.293). ROC curve analysis and box plots for the above parameters are given in Figures 5 and 6, respectively.

Prediction of muscle invasion

p-values generated from the Mann–Whitney U test were statistically significant in distinguishing muscle invasive from non-muscle invasive tumors for 19 parameters (five on T_2WI, six on DWI b1500 and 8 on the ADC images) (Table 5). However, on ROC curve analysis, the only parameters with AUC >0.8 in predicting muscle invasion were mean and MPP at SSF 0 on the ADC images (AUC: 0.819; 95% CI: 0.665–0.922; optimal cut-off:<930.5 x 10^{-3} mm^2/s) (Table 6). As expected, Pearson's test showed perfect linear correlation between these two parameters (r: 1.0). However, since all the muscle invasive tumors in our population were high-grade, it was possible that these texture parameters merely reflected the confounding effect of the high-grade histology of these tumors. Confirming this suspicion, Pearson's test showed perfect correlation (r: 1.0) between the mean/ MPP values (at SSF 0 on the ADC images) of high-grade tumors and those of the muscle invasive tumors. Hence, it was concluded that no texture parameters independent of those which reflected high histologic grade, showed high class separation capacity in differentiating muscle invasive from non-muscle invasive tumors.

DISCUSSION

High histologic grade and presence of muscle invasion are important prognostic factors which guide the treatment of UBC. At present, this information is obtained through TURBT, which is invasive. There exists an unmet need for non-invasive

Figure 4. Dots plots representing intraclass correlation between the measurements extracted by the two readers (R1 and R2) for each of the six texture features (mean, standard deviation, entropy, mean of positive pixels, skewness and kurtosis).

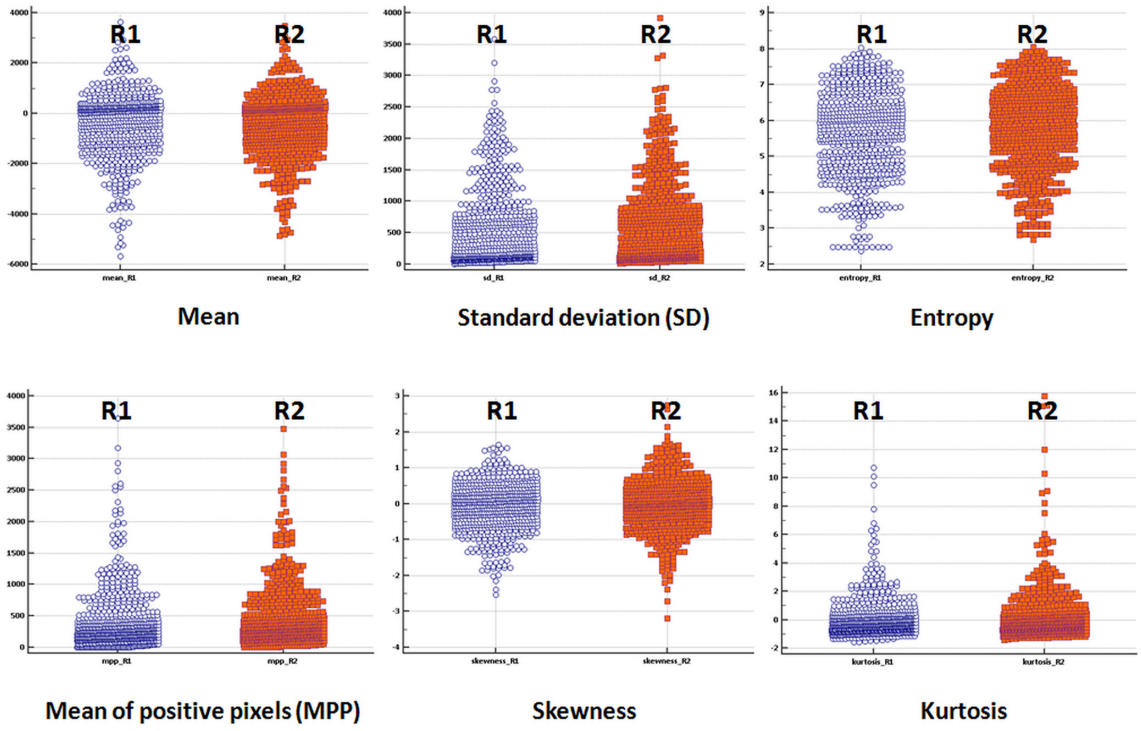

Table 3. Mann–Whitney *U* test in the differentiation of high-grade from low-grade urinary bladder cancer: *p*-values of all the parameters, listed MR sequence-wise

SSF	Mean	SD	Entropy	MPP	Skewness	Kurtosis
T2W						
0	0.272	0.807	0.713	0.272	0.196	0.518
2	0.205	0.503	0.878	0.101	**0.012**	**0.017**
3	0.257	0.546	0.899	0.791	**0.014**	**0.031**
4	0.286	0.807	0.708	0.381	0.296	0.409
5	0.351	0.858	0.574	0.518	0.596	0.679
6	0.568	0.858	0.487	0.994	0.960	0.728
DWI b 1500						
0	0.462	0.218	0.381	0.462	0.407	0.665
2	0.782	0.317	0.827	0.987	0.339	0.996
3	0.782	0.419	0.987	0.935	0.573	0.776
4	0.909	0.546	0.934	0.987	0.942	0.127
5	0.987	0.524	0.935	0.935	0.540	**0.005**
6	0.909	0.462	0.974	0.782	0.765	**0.004**
ADC						
0	**0.000**	0.961	0.791	**0.000**	0.573	0.398
2	0.832	0.334	1.000	0.289	**0.047**	0.363
3	0.807	0.482	0.960	0.398	**0.041**	0.246
4	0.909	0.636	0.960	0.707	0.104	**0.034**
5	0.590	0.757	0.960	0.807	0.426	**0.001**
6	0.286	0.961	0.948	0.988	0.202	**0.046**

MPP, mean of positive pixels; SD, standard deviation; SSF, spatial scale factor.
The statistically significant parameters are shown in bold text.

biomarkers capable of providing this information accurately. Among the novel tools used in quantitative imaging, radiomics and TA have attracted significant interest with several studies having used TA on both CT and MRI images to predict histologic grade and muscle invasion in UBC.[9–15]

We investigated the role of first-order TA parameters on MRI in predicting histologic grade and presence of muscle invasion. MRI was preferred over CT since the higher intrinsic tissue contrast of MRI enables better differentiation of tumor from the bladder wall. MRI also possesses multiple paradigms for the morphologic (*e.g.* T_1WI, T_2WI) and functional (*e.g.*, DWI) assessment of tumors. Hence, TA on MRI may provide more robust results in tumor characterization than CT. All the studies which evaluated TA on MRI till date for staging and grading of UBC assessed numerous higher-order statistical parameters.[12–15] Although these higher-order parameters may have better discriminative capability, the large dimensions of data involved make calculations too complex and computationally intensive for practical and clinical purposes. First-order parameters have also been observed to be more reproducible than higher order parameters, with entropy being the most stable feature.[17] This is relevant since the question of reproducibility across different scanners, acquisition parameters and segmentation techniques is the most significant barrier in the development of prediction models for routine clinical implementation. The generation of numerous texture features from a single data set can result in significant inflation of type-I error, which may be overlooked unless a validation data set is used.[18] Also, the biological basis and pathologic correlates of first-order parameters are better understood than those of higher-order features, the causality of which are difficult to infer.[19–21] For these reasons, only first-order parameters were assessed in this study. We also confirmed the reproducibility of our segmentation technique by observing excellent interobserver correlation across the two readers who extracted the data.

In this study, two parameters (mean/MPP at SSF 0 and kurtosis at SSF 5 on the ADC images) showed excellent class separation capacity in the differentiation of high-grade from low-grade tumors. High-grade tumors showed significantly lower mean/MPP values on the unfiltered ADC images. This finding is attributable to the marked cellularity of high-grade tumors, which restricts free diffusion of water molecules in the interstitial space and results in low signal intensity on the ADC map images. The presence of a significant difference between the ADC values of low-grade and high-grade tumors is a well-established fact.[7,22,23] A similar observation of significantly lower ADC in high-grade tumors was also made in our previously published study.[16]

Table 4. AUC and optimal cut-off values of the statistically significant parameters ($p < 0.05$) in the differentiation of high-grade from low-grade urinary bladder cancer, listed MR sequence-wise

Parameter	SSF	AUC	95% CI	Cut-off	Sensitivity	Specificity
T_2W						
Skewness	2	0.748	0.585–0.871	≤−0.930	68.97	81.82
Skewness	3	0.727	0.564–0.856	≤−0.479	75.86	72.73
Kurtosis	2	0.712	0.547–0.844	≥2.009	41.38	100
Kurtosis	3	0.693	0.527–0.829	≥0.270	41.38	100
DWI b1500						
Kurtosis	5	0.779	0.620–0.895	≥−0.379	58.62	100
Kurtosis	6	0.752	0.591–0.875	≥−0.560	65.52	81.82
ADC						
Mean	0	**0.897**	0.759–0.970	≤963.479	79.31	100
MPP	0	**0.897**	0.759–0.970	≤963.479	79.31	100
Skewness	2	0.702	0.537–0.836	≤−0.519	65.52	81.82
Skewness	3	0.721	0.557–0.851	≤−0.460	65.52	90.91
Kurtosis	4	0.704	0.539–0.837	≥−0.280	48.28	90.91
Kurtosis	5	**0.828**	0.675–0.928	≥−0.579	79.31	81.82
Kurtosis	6	0.712	0.547–0.844	≥−0.730	72.41	72.73

AUC, area under curve; CI, confidence interval; MPP, mean of positive pixels; SSF, spatial scale factor.
Parameters with AUC >0.8 are shown in bold text.

Although there is some overlap in the patient population between the two studies, the techniques used (TA *vs* simple mean ADC estimation) and the methods of ROI placement were completely different. However, no comparable results were observed on the corresponding DWI b1500 images. This could have occurred since ADC value, which is a measure of the slope of signal intensity interpolated across multiple b-values, is a more precise and quantifiable representation of true diffusion restriction than a single b-value DWI trace image. In addition, TA results on the filtered ADC maps (SSF 2–6) failed to show similar results as the unfiltered images. This raises the possibility that filtration, which was originally intended to enhance features and mitigate photon noise, could in turn introduce a type II error when applied to parametric maps. High-grade tumors also showed higher kurtosis values, suggestive of higher peakedness of the histogram. This implies the presence of an identical pattern of restricted diffusion across pixels within the measured ROI.

In the prediction of muscle invasion, only one parameter (mean/MPP at SSF 0 on the ADC images) showed high class separation

Figure 5. ROC curve analysis results for the two texture parameters which showed high class separation capacity (AUC >0.8) in differentiating high-grade from low-grade tumors: (A) Mean/ MPP at SSF 0 and (B) Kurtosis at SSF 5 on the ADC images. ADC, apparent diffusion coefficient; AUC, area under the curve; MPP, mean of positive pixels; ROC, receiver operating characteristic; SSF, spatial scale factor.

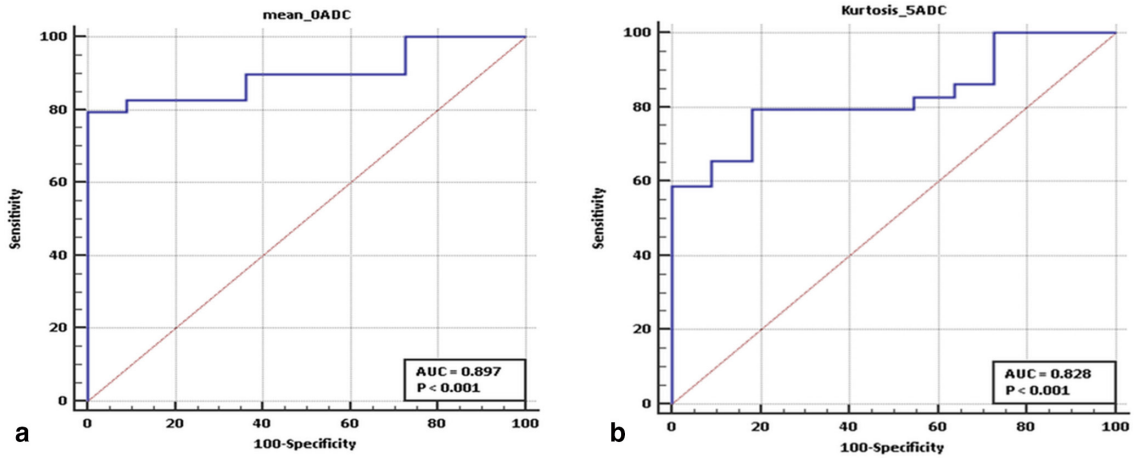

Figure 6. Box and whisker plots of the two texture parameters which showed high class separation capacity (AUC >0.8) in differentiating high-grade from low-grade tumors: (A) Mean/ MPP at SSF 0 and (B) Kurtosis at SSF 5 on the ADC images. The Y-axis represents mean ADC (x 10^{-6} mm^2/s) in panel A and kurtosis in panel B. ADC, apparent diffusion coefficient; AUC, area under the curve; MPP, mean of positive pixels; ROC, receiver operating characteristic; SSF, spatial scale factor.

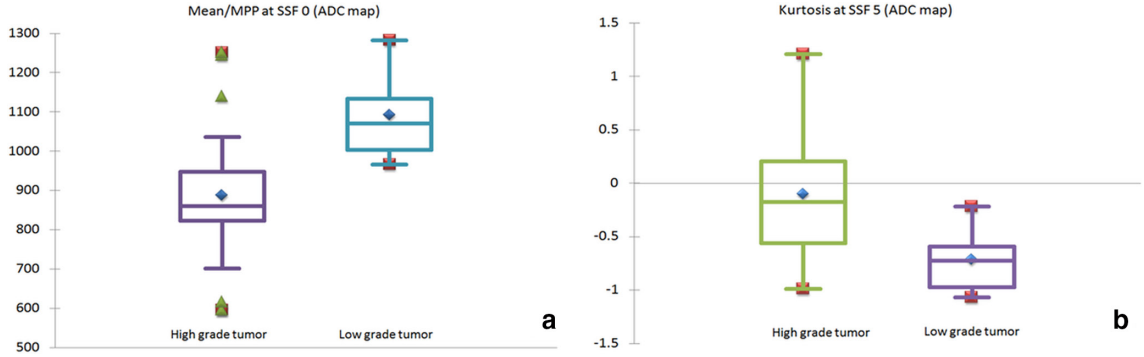

capacity. However, this resulted from the confounding effect of high-grade tumor histology since all the muscle invasive tumors were of high-grade. This possibility was confirmed by the perfect correlation observed between the texture parameters of high-grade and muscle invasive tumors. Hence, no texture features independent of those which reflected high histologic grade, showed high class separation capacity in the differentiation of muscle invasive from non-muscle invasive tumors.

There are a few limitations of this study. Our sample size of 40 tumors was small and a larger number of patients would be required to produce more robust results. Our small sample size

Table 5. Mann–Whitney *U* test in the differentiation of muscle invasive from non-muscle invasive urinary bladder cancer: *p*-values of all the parameters, listed MR sequence-wise

SSF	Mean	SD	Entropy	MPP	Skewness	Kurtosis
T_2W						
0	0.315	0.940	0.423	0.315	0.095	0.076
2	**0.021**	0.223	0.904	0.361	0.080	0.077
3	**0.050**	0.235	0.820	0.785	**0.006**	**0.028**
4	0.100	0.665	0.988	0.964	**0.023**	0.276
5	0.287	0.870	0.868	0.844	0.083	0.372
6	0.463	0.893	0.809	0.515	0.270	0.389
DWI b 1500						
0	0.058	**0.006**	0.082	0.058	0.397	0.586
2	0.754	**0.027**	0.204	1.000	0.079	0.250
3	0.893	**0.030**	0.276	0.777	0.112	0.832
4	0.870	**0.043**	0.289	0.800	0.150	0.762
5	0.893	**0.034**	0.260	0.709	0.372	0.468
6	0.754	**0.016**	0.215	0.520	0.364	0.639
ADC						
0	**0.001**	0.777	0.303	**0.001**	0.762	0.535
2	0.135	0.601	0.458	0.880	**0.020**	**0.035**
3	0.171	0.315	0.380	0.739	**0.008**	0.178
4	0.287	0.361	0.364	0.621	**0.003**	0.397
5	0.665	0.482	0.325	0.820	**0.009**	0.348
6	0.560	0.410	0.296	0.559	**0.013**	0.596

MPP, mean of positive pixels; SD, standard deviation; SSF, spatial scale factor.
The statistically significant parameters are shown in bold text.

Table 6. AUC and optimal cut-off values of the statistically significant parameters ($p < 0.05$) in the differentiation of muscle invasive from non-muscle invasive urinary bladder cancer, listed MR sequence-wise

Parameter	SSF	AUC	95% CI	Cut-off	Sensitivity	Specificity
T2W						
Mean	2	0.701	0.536–0.835	≥−273.109	60.00	80.00
Mean	3	0.669	0.503–0.810	≥−617.830	66.67	80.00
Skewness	3	0.733	0.570–0.860	≤−0.709	66.67	80.00
Skewness	4	0.696	0.530–0.831	≤−0.259	73.33	68.00
Kurtosis	3	0.675	0.508–0.814	≥0.270	60.00	88.00
DWI b1500						
SD	0	0.789	0.631–0.902	≥25.729	93.33	56.00
SD	2	0.741	0.579–0.867	≥101.309	60.00	88.00
SD	3	0.739	0.576–0.864	≥149.639	60.00	88.00
SD	4	0.725	0.561–0.854	≥193.979	53.33	92.00
SD	5	0.736	0.573–0.862	≥137.990	80.00	68.00
SD	6	0.76	0.599–0.881	≥145.130	80.00	72.00
ADC						
Mean	0	**0.819**	0.665–0.922	≤930.5	86.67	72.00
MPP	0	**0.819**	0.665–0.922	≤930.5	86.67	72.00
Skewness	2	0.729	0.566–0.857	≤−0.519	80	64.00
Skewness	3	0.757	0.596–0.879	≤−0.589	66.67	84.00
Skewness	4	0.773	0.614–0.890	≤−0.270	80	80.00
Skewness	5	0.744	0.582–0.869	≤−0.129	73.33	80.00
Skewness	6	0.751	0.589–0.874	≤0.079	73.33	84.00
Kurtosis	2	0.688	0.522–0.825	≥−0.289	80.00	60.00

AUC, area under curve; CI, confidence interval; MPP, mean of positive pixels; SD, standard deviation; SSF, spatial scale factor.
Parameters with AUC >0.8 are shown in bold text.

also limited the incorporation of machine learning techniques which could have helped in generating better classifiers. Intuitively, although whole tumor assessment would have provided more representative data, we limited ourselves to 2D (single slice) ROI placement since volumetric assessment is cumbersome, results in confounding errors from volume averaging and inclusion of hemorrhage/ necrosis, and is less likely to be reproducible across observers.[19] Thirdly, although we accounted for interobserver variability in ROI placement by confirming excellent ICC between the two readers, reproducibility across different scanners and imaging acquisition protocols were not assessed. This could limit the generalizability of our findings. We also did not perform TA of the normal bladder wall, which could have served as an internal reference. Lastly, the reference standard in a significant number of our patients was the TURBT specimen. Since TURBT is known to undersample the tumor and miss muscle invasion, this reference standard may have been imperfect.[24]

In conclusion, our study revealed two first-order texture parameters (mean/MPP at SSF 0 and kurtosis at SSF 5 on the ADC images) which showed excellent class separation capacity in differentiating high-grade from low-grade tumors. Similar diagnostic performance was not seen with the filtered images. No texture parameters independent of those which predicted histologic grade were observed to be useful in the differentiation of muscle invasive from non-muscle invasive tumors. All the texture parameters were reproducible across the two readers. Larger validation studies are required and uniform acquisition protocols need to be adopted before TA can be used in the routine management of UBC patients.

AUTHOR CONTRIBUTIONS

Study concepts and design: A.R., C.J.D., R.S.; Data acquisition: A.R., S.M.; Data analysis and interpretation: A.R., C.J.D., R.S., S.M., S.S., A.S., D.N.S.; Literature research: A.R., C.J.D., R.S.; Manuscript drafting: A.R.; Manuscript revision for important intellectual content: A.R., C.J.D., R.S.; Approval of the final version of the submitted manuscript: all authors.

REFERENCES

1. Richters A, Aben KKH, Kiemeney LALM. The global burden of urinary bladder cancer: an update. *World J Urol* 2020; **38**: 1895–904. doi: https://doi.org/10.1007/s00345-019-02984-4
2. Svatek RS, Hollenbeck BK, Holmäng S, Lee R, Kim SP, Stenzl A, et al. The economics of bladder cancer: costs and considerations of caring for this disease. *Eur Urol* 2014; **66**: 253–62. doi: https://doi.org/10.1016/j.eururo.2014.01.006
3. Pham H, Torres H, Sharma P. Mental health implications in bladder cancer patients: a review. *Urol Oncol* 2019; **37**: 97–107. doi: https://doi.org/10.1016/j.urolonc.2018.12.006
4. Cheung G, Sahai A, Billia M, Dasgupta P, Khan MS. Recent advances in the diagnosis and treatment of bladder cancer. *BMC Med* 2013; **11**: 13. doi: https://doi.org/10.1186/1741-7015-11-13
5. Traxer O, Pasqui F, Gattegno B, Pearle MS. Technique and complications of transurethral surgery for bladder tumours. *BJU Int* 2004; **94**: 492–6. doi: https://doi.org/10.1111/j.1464-410X.2004.04990.x
6. Wang H, Luo C, Zhang F, Guan J, Li S, Yao H, et al. Multiparametric MRI for bladder cancer: validation of VI-RADS for the detection of detrusor muscle invasion. *Radiology* 2019; **291**: 668–74. doi: https://doi.org/10.1148/radiol.2019182506
7. Takeuchi M, Sasaki S, Ito M, Okada S, Takahashi S, Kawai T, et al. Urinary bladder cancer: diffusion-weighted MR imaging--accuracy for diagnosing T stage and estimating histologic grade. *Radiology* 2009; **251**: 112–21. doi: https://doi.org/10.1148/radiol.2511080873
8. Ganeshan B, Miles KA. Quantifying tumour heterogeneity with CT. *Cancer Imaging*. 2013; **13**. :: 140–9Published2013;13(1). doi: https://doi.org/10.1102/1470-7330.2013.0015
9. Zhang G-M-Y, Sun H, Shi B, Jin Z-Y, Xue H-D. Quantitative CT texture analysis for evaluating histologic grade of urothelial carcinoma. *Abdom Radiol* 2017; **42**: 561–8. doi: https://doi.org/10.1007/s00261-016-0897-2
10. Liu ZH, Shi JY, Wang HY, Ye HY, Wang ZB, Yang T, et al. Ct texture analysis in bladder carcinoma: histologic grade characterization. *Zhonghua Zhong Liu Za Zhi* 2018; **40**: 379–83. doi: https://doi.org/10.3760/cma.j.issn.0253-3766.2018.05.011
11. Wang Z, He Y, Wang N, Zhang T, Wu H, Jiang X, et al. Clinical value of texture analysis in differentiation of urothelial carcinoma based on multiphase computed tomography images. *Medicine* 2020; **99**: e20093. doi: https://doi.org/10.1097/MD.0000000000020093
12. Xu X, Liu Y, Zhang X, Tian Q, Wu Y, Zhang G, et al. Preoperative prediction of muscular invasiveness of bladder cancer with radiomic features on conventional MRI and its high-order derivative maps. *Abdom Radiol* 2017; **42**: 1896–905. doi: https://doi.org/10.1007/s00261-017-1079-6
13. Zhang X, Xu X, Tian Q, Li B, Wu Y, Yang Z, et al. Radiomics assessment of bladder cancer grade using texture features from diffusion-weighted imaging. *J Magn Reson Imaging* 2017; **46**: 1281–8. doi: https://doi.org/10.1002/jmri.25669
14. Xu X, Zhang X, Tian Q, Wang H, Cui L-B, Li S, et al. Quantitative identification of Nonmuscle-Invasive and muscle-invasive bladder carcinomas: a multiparametric MRI Radiomics analysis. *J Magn Reson Imaging* 2019; **49**: 1489–98. doi: https://doi.org/10.1002/jmri.26327
15. Xu S, Yao Q, Liu G, Jin D, Chen H, Xu J, et al. Combining DWI radiomics features with transurethral resection promotes the differentiation between muscle-invasive bladder cancer and non-muscle-invasive bladder cancer. *Eur Radiol* 2020; **30**: 1804–12. doi: https://doi.org/10.1007/s00330-019-06484-2
16. Razik A, Das CJ, Sharma S, Seth A, Srivastava DN, Mathur S, et al. Diagnostic performance of diffusion-weighted MR imaging at 3.0 T in predicting muscle invasion in urinary bladder cancer: utility of evaluating the morphology of the reactive tumor stalk. *Abdom Radiol* 2018; **43**: 2431–41. doi: https://doi.org/10.1007/s00261-018-1458-7
17. Traverso A, Wee L, Dekker A, Gillies R. Repeatability and reproducibility of radiomic features: a systematic review. *Int J Radiat Oncol Biol Phys* 2018; **102**: 1143–58. doi: https://doi.org/10.1016/j.ijrobp.2018.05.053
18. Chalkidou A, O'Doherty MJ, Marsden PK. False discovery rates in PET and CT studies with texture features: a systematic review. *PLoS One* 2015; **10**: e0124165. doi: https://doi.org/10.1371/journal.pone.0124165
19. Miles KA, Ganeshan B, Hayball MP. Ct texture analysis using the filtration-histogram method: what do the measurements mean? *Cancer Imaging* 2013; **13**: 400–6. doi: https://doi.org/10.1102/1470-7330.2013.9045
20. Lubner MG, Smith AD, Sandrasegaran K, Sahani DV, Pickhardt PJ. Ct texture analysis: definitions, applications, biologic correlates, and challenges. *Radiographics* 2017; **37**: 1483–503. doi: https://doi.org/10.1148/rg.2017170056
21. Gillies RJ, Kinahan PE, Hricak H. Radiomics: images are more than pictures, they are data. *Radiology* 2016; **278**: 563–77. doi: https://doi.org/10.1148/radiol.2015151169
22. Wang H-jun, Pui MH, Guo Y, Li S-rong, Guan J, Zhang X-ling, Wang H, Li S, Zhang X, et al. Multiparametric 3-T MRI for differentiating Low-Versus high-grade and category T1 versus T2 bladder urothelial carcinoma. *American Journal of Roentgenology* 2015; **204**: 330–4. doi: https://doi.org/10.2214/AJR.14.13147
23. Yoshida S, Takahara T, Kwee TC, Waseda Y, Kobayashi S, Fujii Y. Dwi as an imaging biomarker for bladder cancer. *American Journal of Roentgenology* 2017; **208**: 1218–28. doi: https://doi.org/10.2214/AJR.17.17798
24. Herr HW. The value of a second transurethral resection in evaluating patients with bladder tumors. *J Urol* 1999; **162**: 74–6. doi: https://doi.org/10.1097/00005392-199907000-00018